Underwater Acoustic Channel Estimation Based on Sparsity-Aware Deep Neural Networks

Longjie Gao, Sicong Liu*, *Member, IEEE*
Department of Information and Communication Engineering, School of Informatics, Xiamen University
Xiamen, China
liusc@xmu.edu.cn

***Abstract*—The estimation of the underwater acoustic channel (UAC) is a difficult problem in underwater acoustic orthogonal frequency division multiplexing (UA-OFDM) systems due to the detrimental characteristics of the UAC, including severe multipath fading, Doppler spread, and large transmission delay, etc. To overcome the problems and improve the performance of UAC estimation, a deep-learning-based approach utilizing a sparsity-aware deep neural network (DNN) emulating the sparse recovery algorithm of approximate message passing (AMP) is proposed for UAC estimation in this paper. The proposed method called Sparsity-Aware-DNN-based UAC Estimation (SAD-UACE) decomposes the conventional iterative sparse recovery algorithm of AMP into several differently parameterized layers of a DNN to learn the inherent sparse structure of the UAC, so that the accuracy of estimation can be improved, especially in severe conditions of underwater acoustic communications. Simulation results show that the proposed SAD-UACE method can significantly improve the accuracy and spectral efficiency of UAC estimation, compared with other state-of-the-art methods, especially in severe conditions of low SNR or insufficient pilots.**

***Index Terms*—underwater acoustic channel, OFDM, sparse channel estimation, deep learning, deep neural networks**

I. Introduction

In recent decades, the application fields of underwater acoustic communications have been increasingly widely, mainly including the exploration of oceanographic science, the monitoring of marine environment, the acquisition of marine resources, and the application of marine military, etc [1]. This has led to a growing demand for underwater acoustic communications [2]. However, due to the fluctuation of water surface, the interference of ambient noise, and the movement of transmitter or receiver, the UAC has many complicated characteristics, such as time varying, multipath fading, delay spread, and Doppler spread, etc. [3], which seriously affect the performance of underwater acoustic communication systems, such as inter-symbol interference (ISI) [4]. Consequently, the multi-carrier modulation scheme of orthogonal frequency division multiplexing (OFDM) has been widely used in underwater acoustic communication systems due to the high spectral efficiency and the robustness to multipath fading [5].

In underwater acoustic communications, channel estimation is aimed to obtain the channel state information (CSI) of the UAC for equalization to improve the performance of underwater acoustic communication systems. The complicated characteristics of the UAC lead to a large number of parameters to be estimated. Fortunately, the channel impulse response (CIR) of the UAC is sparse, i.e. the channel energy is mainly concentrated in only a few paths [6], [7]. Therefore, exploiting the sparsity of the UAC is the key to improving the performance of channel estimation.

Currently, the UAC estimation methods mainly include two categories, i.e. the traditional methods and the compressed sensing (CS) based methods. The traditional methods include the least square (LS) [8] and the minimum mean square error (MMSE) [9] methods, etc. However, the sparsity of the UAC is not utilized effectively, so the performance is limited [8]. The CS-based methods are mainly related to convex optimization algorithms and greedy algorithms. Some of the methods based on convex optimization algorithms use l_1 norm constraint to estimate the channel, such as the approximate message passing (AMP) [10] and the iterative shrinkage threshold (ISTA) [11] algorithms, etc. The methods based on greedy algorithms include orthogonal matching pursuit (OMP) and many related improved greedy algorithms [12]–[15]. The sparse adaptive matching pursuit algorithm (SAMP) proposed in [16] does not require the prior information of the sparsity, thus improving the estimation stability of different sparsity. Although the sparsity is exploited by CS-based algorithms, the performance will be degraded, especially in severe conditions like low SNR or insufficient measurement data [17]–[20].

With the development of deep learning (DL) techniques, they have been widely applied in many fields, such as sparse recovery [21] and massive MIMO enabled communications [22]–[24]. Meanwhile, the endeavour to utilize deep learning and DNN for sparse learning of the UAC remains to be well explored yet. Consequently, in order to solve the problems of existing UAC estimation methods, a Sparsity-Aware-DNN-based UAC Estimation (SAD-UACE) method is proposed for the estimation of the UAC, which exploits the inherent sparse feature of the UAC using deep learning. The main contributions of this paper are summarized in the following two points:

- A DL-based UAC estimation method is proposed in this paper, which decomposes the iterative AMP algorithm into several layers of a sparsity-aware DNN, for deep learning of the sparse structure of the UAC. Since the

This work is supported in part by the National Natural Science Foundation of China under grants 61901403, 61971366, and 61971365, in part by the Youth Innovation Fund of Xiamen under grant 3502Z20206039, and in part by the Natural Science Foundation of Fujian Province of China under grant 2019J05001. (*Corresponding author: Sicong Liu*).

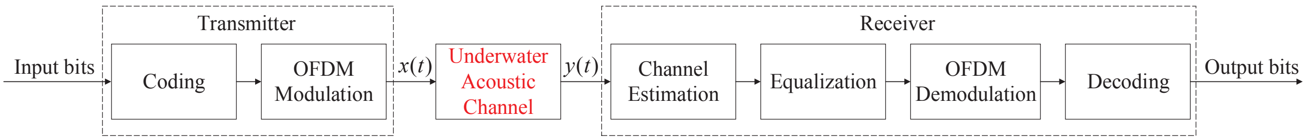

Fig. 1. Block diagram of the typical UA-OFDM system.

parameters of each layer of the DNN emulating the AMP iterations are learnable, the proposed SAD-UACE method has a higher degree of freedom and can thus adapt to the UAC with different sparsity in various severe conditions.

- The CIR of the UAC can be estimated with high accuracy by only a one-way feed-forward calculation in the well-trained sparsity-aware DNN to obtain the sparse support followed by a simple LS method to get the amplitude. The simulation results show that, compared with other state-of-the-art methods, the accuracy and spectral efficiency of UAC estimation have been greatly improved.

The remainder of this paper is organized as follows: the UA-OFDM system model is presented in Section II; Section III introduces the SAD-UACE method proposed in this paper; Section IV reports the simulation results and discussions. Finally, this paper is concluded in section V.

II. System Model

The block diagram of a typical UA-OFDM system is shown in Fig. 1. We can use $h\left(t;\tau\right)$ to represent the CIR of the underwater acoustic channel, where t and τ denote the time and delay, respectively. The signal transmission relationship can be expressed as [25], [26]

$$\begin{aligned} y(t) &= x(t) * h(t;\tau) + n(t) \\ &= \int h(t;\tau) x(t-\tau) d\tau + n(t) \ , \end{aligned} \tag{1}$$

where $x\left(t\right)$ and $y\left(t\right)$ denote the transmitted passband signal and the received passband signal, respectively. $n\left(t\right)$ denotes the additive noise in passband and $*$ denotes the convolution operation.

As a block transmission scheme, the cyclic prefix OFDM (CP-OFDM) is adopted in this paper [6]. Let T denote the duration of one OFDM symbol and let T_{CP} denote the length of the cyclic prefix (CP), and then the total block duration T_{bl} corresponding to an OFDM block is equal to $T_{\mathrm{CP}} + T$.

Assume that there are N subcarriers in one OFDM block. The kth subcarrier is located at the frequency given by

$$f_{\mathrm{k}} = f_{\mathrm{c}} + \frac{k}{T}, \quad k = -\frac{N}{2}, \cdots, \frac{N}{2} - 1 \ , \tag{2}$$

where f_{c} is the center frequency of the carrier.

Let $s\left[k\right]$ denote the transmitted symbol on the kth subcarrier and let S_{A} denote the set of actively transmitted subcarriers. The transmitted passband signal is then represented as

$$x(t) = \mathbf{Re}\left\{ \sum_{k\in S_{\mathrm{A}}} s[k] \mathrm{e}^{\mathrm{j}2\pi f_{\mathrm{k}} t} \right\}, \quad t \in [-T_{\mathrm{CP}}, T] \ . \tag{3}$$

where $\mathbf{Re}\left\{\cdot\right\}$ denotes the real part operator.

After passing through a specific underwater acoustic channel, the expression of the received passband signal within the interval $[0, T]$ is given by

$$\begin{aligned} r(t) &= \int_0^{T_{\mathrm{h}}} h(\tau) \mathbf{Re}\left\{ \sum_{k\in S_{\mathrm{A}}} s[k] \mathrm{e}^{\mathrm{j}2\pi f_{\mathrm{k}}(t-\tau)} \right\} d\tau + n(t) \\ &= \mathbf{Re}\left\{ \sum_{k\in S_{\mathrm{A}}} H\left(f_{\mathrm{k}}\right) s[k] \mathrm{e}^{\mathrm{j}2\pi f_{\mathrm{k}} t} \right\} + n(t) \ , \end{aligned} \tag{4}$$

where T_{h} denotes the duration of $h\left(t\right)$ and $H\left(f_{\mathrm{k}}\right)$ denotes the channel frequency response.

In general, the CIR of the time varying UAC can be represented as [25]–[27]

$$h(t;\tau) = \sum_{p=1}^{L} A_{\mathrm{p}}(t) \delta\left(\tau - \tau_{\mathrm{p}}(t)\right) \ , \tag{5}$$

where L denotes the number of multipath. $A_{\mathrm{p}}\left(t\right)$ and τ_{p} are the time varying amplitude and delay for the pth path, respectively.

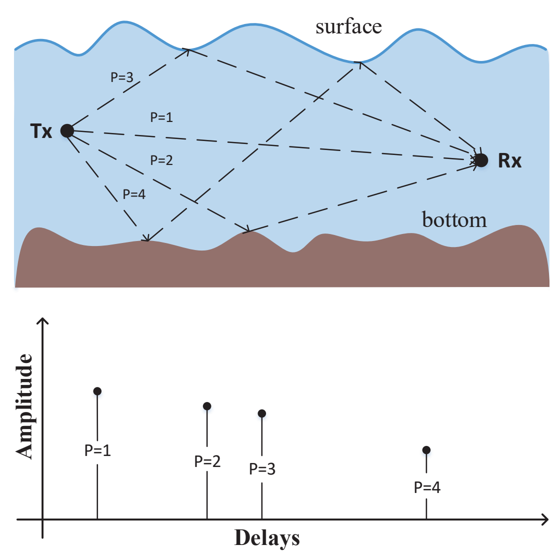

Fig. 2. Multipath propagation in a shallow water environment.

Fig. 2 shows a diagram of multipath propagation in a shallow water environment. For UAC, the amplitude of the dominant K paths are non-zero, and the amplitude of other paths are zero or approximately zero compared with the dominant paths, since that the CIR is sparse [3], [26]. The sparsity is K, with $K \ll L$ usually.

Within the duration T_{bl} of one OFDM symbol, we can adopt the following assumptions commonly recognized in UAC [28]:

- The amplitude of each path is constant, i.e. $A_{\mathrm{p}}(t) = A_{\mathrm{p}}$.
- The delay variation of each path can be approximated by the Doppler scale factor as
$$\tau_{\mathrm{p}}(t) \approx \tau_{\mathrm{p}} - a_{\mathrm{p}} t, \quad t \in [0, T_{\mathrm{bl}}] \ , \tag{6}$$
where the constant τ_{p} is the initial delay, and a_{p} denotes the Doppler scale factor.

Therefore, the UAC model can be modeled as

$$h(t;\tau) = \sum_{p=1}^{L} A_{\mathrm{p}} \delta\left(\tau - (\tau_{\mathrm{p}} - a_{\mathrm{p}} t)\right) \ . \tag{7}$$

Then the received passband signal can be represented as

$$\begin{aligned} r(t) &= \sum_{p=1}^{L} A_{\mathrm{p}} x\left((1+a_{\mathrm{p}})\, t - \tau_{\mathrm{p}}\right) + n(t) \\ &= \mathbf{Re}\left\{ \sum_{p=1}^{L} A_{\mathrm{p}} \left\{ \sum_{k \in S_{\mathrm{A}}} s[k]\, \mathrm{e}^{\mathrm{j}2\pi f_{\mathrm{k}}((1+a_{\mathrm{p}})t - \tau_{\mathrm{p}})} \right\} \right\} + n(t). \end{aligned} \tag{8}$$

Adopting a two-step Doppler compensation operation for $r(t)$ just as what is done in [25], the received signal after resampling operation can be expressed as

$$\begin{aligned} y(t) &= r\left(\frac{t}{1+\hat{a}}\right) \mathrm{e}^{-\mathrm{j}2\pi\hat{\varepsilon}t} \\ &\approx \mathbf{Re}\left\{ \sum_{p=1}^{L} A_{\mathrm{p}} \left\{ \sum_{k \in S_{\mathrm{A}}} s[k]\, \mathrm{e}^{\mathrm{j}2\pi f_{\mathrm{k}} t} \right\} \right\} + n(t) \ , \end{aligned} \tag{9}$$

where $\hat{a}$ denotes the resampling factor and $\hat{\varepsilon}$ denotes the estimated residual Doppler shift.

In this paper, we adopt the pilot-assisted channel estimation method, which is performed in the frequency domain. Then according to the vector form of Eq. (9) and the pilot-assisted channel estimation method, the UAC estimation problem can be formulated in the frequency domain as

$$\begin{aligned} \mathbf{Y} &= \mathbf{X}\,\mathbf{H} + \mathbf{N} \\ &= \mathbf{X}\,\mathbf{F}_{\mathrm{p}}\,\mathbf{h} + \mathbf{N} \\ &= \mathbf{A}\,\mathbf{h} + \mathbf{N} \ , \end{aligned} \tag{10}$$

where the channel measurement data $\mathbf{Y} = \left[Y_1, Y_2, Y_3, \cdots, Y_{N_{\mathrm{p}}}\right]^{\mathrm{T}}$ is obtained by the received pilots at the receiver with N_{p} being the number of pilots. $\mathbf{X} = \mathrm{diag}\left(X_1, X_2, X_3, \cdots, X_{N_{\mathrm{p}}}\right)$ is a diagonal matrix with its diagonal elements being the transmitted pilots. $\mathbf{H} = \left[H_1, H_2, H_3, \cdots, H_L\right]^{\mathrm{T}}$ denotes the channel frequency response. $\mathbf{h} = \left[h_1, h_2, h_3, \cdots, h_L\right]^{\mathrm{T}}$ denotes the CIR of the UAC. $\mathbf{F}_{\mathrm{p}}$ denotes the partial DFT matrix with size $N_{\mathrm{p}} \times L$, which is dependent on the position of pilots. $\mathbf{N} = \left[N_1, N_2, N_3, \cdots, N_{N_{\mathrm{p}}}\right]^{\mathrm{T}}$ denotes the additive noise in the frequency domain. The matrix $\mathbf{A}$ is also called the measurement matrix in the framework of sparse recovery, which is given by $\mathbf{A} = \mathbf{X}\mathbf{F}_{\mathrm{p}}$.

III. Proposed Sparsity-Aware-DNN-Based Underwater Acoustic Channel Estimation Method

According to the theory of CS, let $\mathbf{A}$ denote the measurement matrix and let $\mathbf{Y}$ denote the observation vector, then the unknown $\mathbf{h}$ of the UAC can be reconstructed by the CS sparse recovery algorithms. Therefore, the UAC estimation problem in Eq. (10) can be reformulated as a sparse recovery problem [6] and the objective function is written as

$$\min \|\mathbf{h}\|_0, \qquad \text{s.t. } \|\mathbf{Y} - \mathbf{A}\mathbf{h}\|_2 \leqslant \varepsilon \ , \tag{11}$$

where $\|\cdot\|_0$ and $\|\cdot\|_2$ denote the l_0 norm and l_2 norm, respectively. ε is the allowable reconstruction error.

Although the common CS sparse recovery algorithms, such as OMP and AMP, can achieve good results in UAC estimation with little noise influence. However, when under the severe conditions of low SNR or insufficient pilots, the accuracy of estimation is limited [18]. In order to solve the deficiencies of existing methods, using the theory of DL and DNN, a method called SAD-UACE for UAC estimation is proposed, which decomposes the AMP into a DNN to estimate the sparse support of the UAC, thereby improving the accuracy and stability of estimation significantly. The pseudo-code of the proposed SAD-UACE method is summarized in **Algorithm 1**.

Algorithm 1: Sparsity-Aware-DNN-Based Underwater Acoustic Channel Estimation (SAD-UACE).

Input: The observation vector $\mathbf{Y}$, the measurement matrix $\mathbf{A}$, the number of layers T.
Initialization: $M = N_{\mathrm{p}}$, $N = L$, $\mathbf{v}_0 = \mathbf{0}$, $b_0 = 0$, $\widehat{\mathbf{h}}_0 = \mathbf{0}$, $\mathbf{B}_0 = \mathbf{A}^{\mathrm{T}}$, $\mathbf{h}_{\mathrm{SAD}} = \mathbf{0}$.
for $t = 1, 2, 3, \cdots, T$. **do**
  $\mathbf{v}_{\mathrm{t}} = \mathbf{Y} - \mathbf{A}\widehat{\mathbf{h}}_{\mathrm{t\text{-}1}} + b_{\mathrm{t}}\mathbf{v}_{\mathrm{t\text{-}1}}$
  $\sigma_{\mathrm{t}}^2 = \frac{1}{M}\|\mathbf{v}_{\mathrm{t}}\|_2^2$
  $\mathbf{r}_{\mathrm{t}} = \widehat{\mathbf{h}}_{\mathrm{t\text{-}1}} + \mathbf{B}_{\mathrm{t}}\mathbf{v}_t$
  $\widehat{\mathbf{h}}_{\mathrm{t}} = \boldsymbol{\eta}\left(\mathbf{r}_{\mathrm{t}}; \lambda_{\mathrm{t}}, \sigma_{\mathrm{t}}^2\right)$
  $b_{\mathrm{t}} = \frac{1}{M}\left\|\widehat{\mathbf{h}}_{\mathrm{t}}\right\|_0$
  $\lambda_{\mathrm{t}} = \frac{1}{\sqrt{M}}\|\mathbf{v}_{\mathrm{t}}\|_2$
end
$\Omega = \mathbb{S}\left(\widehat{\mathbf{h}}_{\mathrm{t}}, K\right)$
$\mathbf{h}_{\mathrm{SAD}}|_{\Omega} = \mathbf{A}_{\Omega}^{\dagger}\mathbf{Y} = \left(\mathbf{A}_{\Omega}^{\mathrm{H}}\mathbf{A}_{\Omega}\right)^{-1}\mathbf{A}_{\Omega}^{\mathrm{H}}\mathbf{Y}$
Output: estimation result $\mathbf{h}_{\mathrm{SAD}}$.

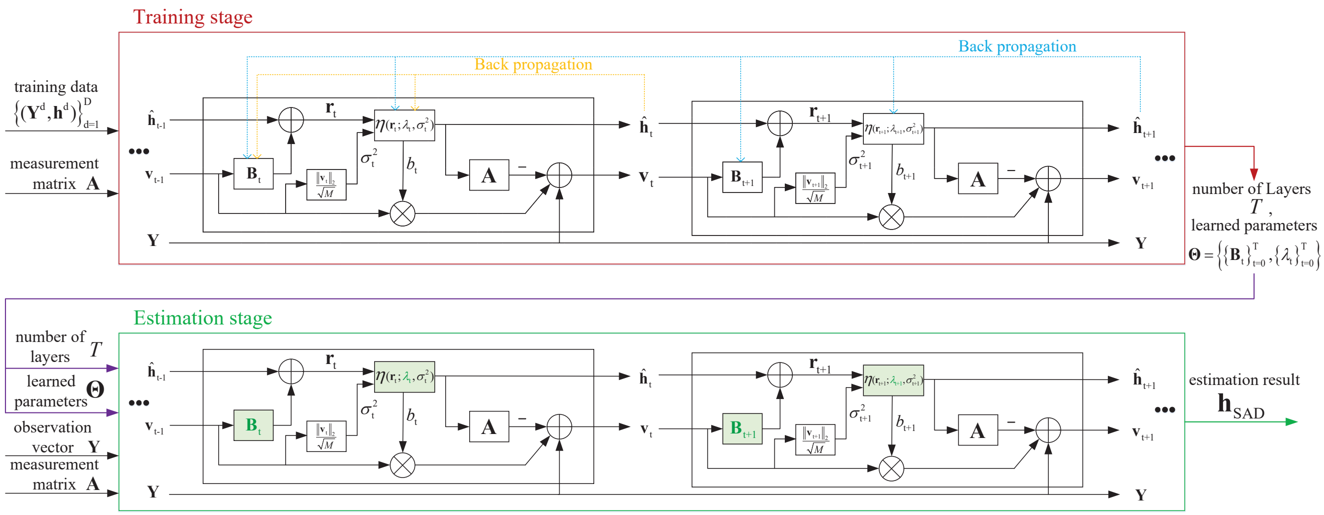

Fig. 3. The training stage and estimation stage of SAD-UACE method.

In Algorithm 1, $\mathbf{v}_{\mathrm{t}}$ denotes the residual measurement error vector of the t-th layer. $b_{\mathrm{t}}\mathbf{v}_{\mathrm{t\text{-}1}}$ is called Onsager Correction [29], which accelerates the convergence. σ_{t} is the estimated value of standard deviation of $\mathbf{v}_{\mathrm{t}}$. $\mathbf{B}_{\mathrm{t}}$ denotes the linear transform matrix of the t-th layer, which is learnable. $\widehat{\mathbf{h}}_{\mathrm{t}}$ denotes the estimation result of the t-th layer. $\boldsymbol{\eta}(\cdot)$ denotes the soft threshold shrinkage function, which is the same for each layer of the DNN. $\boldsymbol{\eta}(\cdot)$ is given by

$$\begin{aligned}\left[\boldsymbol{\eta}\left(\mathbf{r}_{\mathrm{t}};\lambda_{\mathrm{t}},\sigma_{\mathrm{t}}^{2}\right)\right]_{\mathrm{i}}&=\boldsymbol{\eta}\left(\left|r_{\mathrm{t,i}}\right|;\lambda_{\mathrm{t}},\sigma_{\mathrm{t}}^{2}\right)\\&=\operatorname{sgn}\left(r_{\mathrm{t,i}}\right)\max\left(\left|r_{\mathrm{t,i}}\right|-\lambda_{\mathrm{t}}\sigma_{\mathrm{t}},0\right)\ ,\end{aligned}\tag{12}$$

where $r_{\mathrm{t,i}}$ denotes the i-th element of $\mathbf{r}_{\mathrm{t}}$. λ_{t} is learnable threshold shrinkage parameter of $\boldsymbol{\eta}(\cdot)$ of the t-th layer. $(\cdot)^{\dagger}$ and $(\cdot)^{\mathrm{H}}$ denote the Moore-Penrose pseudoinverse and conjugate transpose, respectively. Ω denotes the sparse support of the UAC, which is a set that contains the indices of the K largest entries in $\widehat{\mathbf{h}}_{\mathrm{t}}$. $\mathbf{A}_{\Omega}$ denotes the sub-matrix of matrix $\mathbf{A}$, which consists of the columns of matrix $\mathbf{A}$ indexed by set Ω; $\mathbb{S}\left\{\mathbf{v},K\right\}$ denotes the operation of selecting the indices of the K largest entries in the vector $\mathbf{v}$.

As shown in Fig. 3, utilizing the proposed SAD-UACE method to estimate the CIR of the UAC includes two stages: the training stage and the estimation stage, which are described in **Algorithm 2** and **Algorithm 3**, respectively.

Let $\left\{\left(\mathbf{Y}^{\mathrm{d}},\mathbf{h}^{\mathrm{d}}\right)\right\}_{\mathrm{d=1}}^{\mathrm{D}}$ denote the training data with size D, where $\mathbf{Y}$ and $\mathbf{h}$ are the noisy observation vector and the corresponding truth CIR of the UAC, respectively. The training data $\left\{\left(\mathbf{Y}^{\mathrm{d}},\mathbf{h}^{\mathrm{d}}\right)\right\}_{\mathrm{d=1}}^{\mathrm{D}}$ are composed of (feature,label) pairs, which are used to train the learnable parameters $\boldsymbol{\Theta}=\left\{\left\{\mathbf{B}_{\mathrm{t}}\right\}_{\mathrm{t=0}}^{\mathrm{T}},\left\{\lambda_{\mathrm{t}}\right\}_{\mathrm{t=0}}^{\mathrm{T}}\right\}$ of the DNN. $\mathbf{h}_{\mathrm{SAD}}$ denotes the output of the DNN and the following mean square error (MSE) is used as loss function:

$$L_{\mathrm{T}}(\boldsymbol{\Theta})=\frac{1}{D}\sum_{d=1}^{D}\left\|\mathbf{h}^{\mathrm{d}}-\mathbf{h}_{\mathrm{SAD}}^{\mathrm{d}}\left(\mathbf{Y}^{\mathrm{d}},\boldsymbol{\Theta}\right)\right\|_{2}^{2}\ .\tag{13}$$

Algorithm 2: SAD-UACE - Training stage. (Parameters $\boldsymbol{\Theta}$ learning.)

Input: The training data $\left\{\left(\mathbf{Y}^{\mathrm{d}},\mathbf{h}^{\mathrm{d}}\right)\right\}_{\mathrm{d=1}}^{\mathrm{D}}$, the measurement matrix $\mathbf{A}$.
(Training for each layer of the DNN.)
for $t=1,2,3,\cdots$ **do**
  Initialize $\mathbf{B}_{\mathrm{t}}=\mathbf{A}^{\mathrm{T}}$, $\lambda_{\mathrm{t}}=\lambda_{\mathrm{t\text{-}1}}$.
  Use back propagation update and optimize $\mathbf{B}_{\mathrm{t}}$, λ_{t} jointly through the stochastic gradient descent to minimize the loss function $L(\boldsymbol{\Theta})$ from Eq. (13).
  If $L_{\mathrm{t+1}}(\boldsymbol{\Theta})\geqslant L_{\mathrm{t}}(\boldsymbol{\Theta})$, then set the number of the DNN layers $T\leftarrow t$, **break**.
end
Output: learned parameters $\boldsymbol{\Theta}=\left\{\left\{\mathbf{B}_{\mathrm{t}}\right\}_{\mathrm{t=0}}^{\mathrm{T}},\left\{\lambda_{\mathrm{t}}\right\}_{\mathrm{t=0}}^{\mathrm{T}}\right\}$, the number of layers T .

As depicted in Algorithm 2, in the training stage, the learnable parameters $\boldsymbol{\Theta}$ are trained in a layer-by-layer manner: when we train the t-th layer, all the parameters of the previous layers are kept fixed, add one layer at a time and repeat until we have trained a T layers DNN. The loss function $L_{\mathrm{T}}(\boldsymbol{\Theta})$ decreases with the increase of the number of layers T and the learnable parameters $\boldsymbol{\Theta}$ can be updated and optimized. Using back propagation (BP) and stochastic gradient descent (SGD) to minimize the loss from Eq. (13), when the loss stops decreasing as the increase of the number of layers, i.e. $L_{\mathrm{t+1}}(\boldsymbol{\Theta})\geqslant L_{\mathrm{t}}(\boldsymbol{\Theta})$, since overfitting might occur at this moment, so the optimal number of the DNN layers is $T\leftarrow t$, and the training stage ends.

As depicted in Algorithm 3, in the estimation stage, the well-trained DNN is first used to estimate the CIR of the UAC. Then, the indices of K largest entries in the estimated CIR are selected to estimate the dominant sparse support Ω. Finally, the

Algorithm 3: SAD-UACE - Estimation stage.

1 Input: The observation vector $\mathbf{Y}$, the measurement matrix $\mathbf{A}$, the number of layers T, the learned parameters $\boldsymbol{\Theta}$ obtained in training stage.
2 Initialization: $\mathbf{v}_0 = \mathbf{0}$, $b_0 = 0$, $\widehat{\mathbf{h}}_0 = \mathbf{0}$, $\mathbf{h}_{\text{SAD}} = \mathbf{0}$.
3 Input $\mathbf{Y}$, $\mathbf{A}$ to the T layers DNN with learned parameters $\boldsymbol{\Theta}$ to estimate the CIR $\widehat{\mathbf{h}}_{\text{T}} = \boldsymbol{\eta}\left(\mathbf{r}_{\text{T}}; \lambda_{\text{T}}, \sigma_{\text{T}}^2\right)$.
4 Select the indices of the K largest entries in $\widehat{\mathbf{h}}_{\text{T}}$ to estimate the dominant sparse support $\Omega = \mathbb{S}\left(\widehat{\mathbf{h}}_{\text{T}}, K\right)$.
5 Solve the least square problem: $\mathbf{h}_{\text{SAD}}|_{\Omega} = \mathbf{A}_{\Omega}^{\dagger}\mathbf{Y} = \left(\mathbf{A}_{\Omega}^{\text{H}}\mathbf{A}_{\Omega}\right)^{-1}\mathbf{A}_{\Omega}^{\text{H}}\mathbf{Y}$.
6 Output: estimation result $\mathbf{h}_{\text{SAD}}$.

UAC estimation problem given by Eq. (11) can be simplified to an LS problem to get the amplitude of the non-zero entries of $\mathbf{h}_{\text{SAD}}$ at the sparse support Ω, thereby obtaining the accurate estimation result $\mathbf{h}_{\text{SAD}}$ of the UAC.

Since the sparsity-aware DNN in the proposed SAD-UACE method can learn the sparse structure of the UAC well, the proposed SAD-UACE method can accurately estimate the sparse support of the UAC, thereby significantly improving the accuracy and stability of UAC estimation.

IV. Simulation Results

In this section, we evaluate the performance of the proposed SAD-UACE method through numerical simulations, and compare it with the state-of-the-art methods in UAC estimation under different SNR values and different number of pilots to investigate the performance in different noise conditions and spectrum resources. The main simulation parameters of UA-OFDM system are given in Table I.

TABLE I
Simulation Parameters

Carrier Frequency	12kHz
Bandwith	8kHz
Number of Subcarriers	1024
CP Length	256
Modulation	BPSK
Number of Pilots	64
Environment	shallow water
Sound Velocity	1500m/s
Channel Length	256
Number of Channel Paths	8

In the training stage of the proposed SAD-UACE method, the training data sets $\left\{(\mathbf{Y}^{\text{d}}, \mathbf{h}^{\text{d}})\right\}_{\text{d=1}}^{\text{D}}$ with size D = 2000 are randomly generated and the test data sets are generated in a similar way. The learning rate lr of the parameters $\boldsymbol{\Theta}$ in the DNN is set to 0.001 and the Adam optimizer is utilized to train the DNN. After several training epochs, the optimal number of layers is converged to T = 8, and the optimal parameters $\boldsymbol{\Theta} = \left\{\{\mathbf{B}_{\text{t}}\}_{\text{t=0}}^{\text{T}}, \{\lambda_{\text{t}}\}_{\text{t=0}}^{\text{T}}\right\}$ of the DNN are obtained.

The performance of UAC estimation is evaluated by the normalized mean square error (NMSE), which is defined as

$$\text{NMSE} = \text{E}\left[\frac{\left\|\mathbf{h} - \widehat{\mathbf{h}}\right\|_2^2}{\|\mathbf{h}\|_2^2}\right]. \tag{14}$$

where $\widehat{\mathbf{h}}$ denotes the estimation result, $\|\cdot\|_2$ denotes the l_2 norm, $\text{E}\left[\cdot\right]$ denotes the expectation.

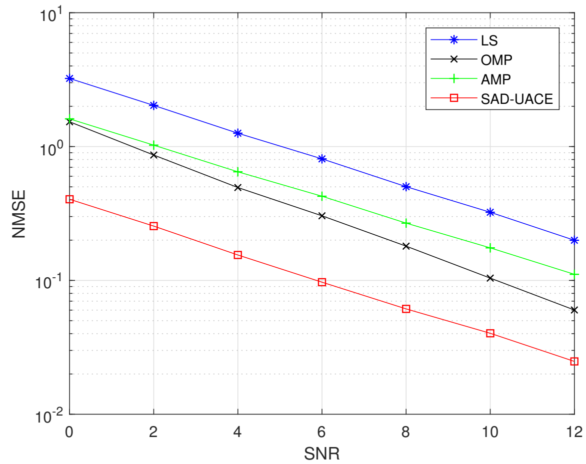

Fig. 4. The performance of the accuracy of channel estimation for UAC versus SNR.

Fig. 4 shows the NMSE performance comparison of different algorithms for UAC estimation with respect to different SNR values using 64 available pilots for channel estimation. The result shows that the proposed SAD-UACE method outperforms the existing methods of LS, AMP, and OMP by approximately 10dB, 6dB, and 4dB, respectively. This shows that the sparsity-aware DNN in the proposed SAD-UACE method has successfully learned the sparse structure of the UAC and estimated the sparse support accurately, so that the accuracy of estimation can be improved, especially in the harsh condition of intensive noise.

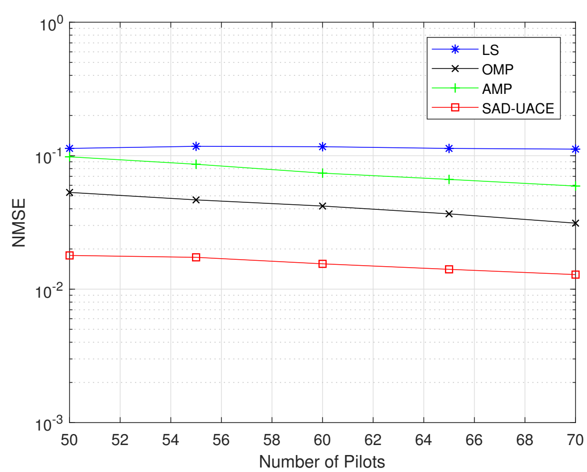

Fig. 5. The performance of UAC estimation with respect to different number of available pilots.

Fig. 5 shows the NMSE performance comparison of different algorithms for UAC estimation under the condition of a different number of pilots with the SNR of 15dB. Compared with the existing methods of LS, OMP, and AMP, the proposed SAD-UACE method can achieve a higher accuracy of UAC estimation with a smaller number of pilots and significantly improve the spectrum efficiency.

V. Conclusion

In this paper, a SAD-UACE method for UAC estimation is proposed, which has higher estimation accuracy and spectral efficiency than the state-of-the-art methods. The inherent sparse feature of the underwater acoustic channels is fully exploited to facilitate the channel estimation by the deep learning over the sparsity-aware DNN, which emulates the iterative sparse recovery algorithm of AMP. The simulation results verify that the proposed SAD-UACE method significantly outperforms other existing methods both in the estimation accuracy and spectrum efficiency, especially in the severe conditions of low SNR or insufficient pilots as measurement data. The proposed method is promising to be applied in many underwater communication scenarios and applications that require accurate and efficient channel estimation.

References

[1] A. C. Singer, J. K. Nelson, and S. S. Kozat, "Signal processing for underwater acoustic communications," *IEEE Commun. Mag.*, vol. 47, no. 1, pp. 90–96, 2009.

[2] A. Radosevic, R. Ahmed, T. M. Duman, J. G. Proakis, and M. Stojanovic, "Adaptive OFDM modulation for underwater acoustic communications: Design considerations and experimental results," *IEEE J. Ocean. Eng.*, vol. 39, no. 2, pp. 357–370, 2014.

[3] P. Chen, Y. Rong, S. Nordholm, Z. He, and A. J. Duncan, "Joint channel estimation and impulsive noise mitigation in underwater acoustic OFDM communication systems," *IEEE Trans. Wireless Commun.*, vol. 16, no. 9, pp. 6165–6178, 2017.

[4] X. Wang, J. Wang, L. He, and J. Song, "Doubly selective underwater acoustic channel estimation with basis expansion model," in *2017 IEEE International Conference on Communications (ICC)*, 2017, pp. 1–6.

[5] K. Tu, D. Fertonani, T. M. Duman, M. Stojanovic, and P. Hursky, "Mitigation of intercarrier interference for OFDM over time-varying underwater acoustic channels," *IEEE J. Ocean. Eng.*, vol. 36, no. 2, pp. 156–171, 2011.

[6] G. Qiao, Q. Song, L. Ma, S. Liu, Z. Sun, and S. Gan, "Sparse Bayesian learning for channel estimation in time-varying underwater acoustic OFDM communication," *IEEE Access*, vol. 6, pp. 56 675–56 684, 2018.

[7] L. Ma, F. Xiao, and M. Li, "Research on time-varying sparse channel prediction algorithm in underwater acoustic channels," in *2019 3rd International Conference on Electronic Information Technology and Computer Engineering (EITCE)*, 2019, pp. 2014–2018.

[8] K. S. Priyanjali and A. V. Babu, "An improved least square channel estimation technique for OFDM systems in sparse underwater acoustic channel," in *2014 International Conference on Advances in Computing, Communications and Informatics (ICACCI)*, 2014, pp. 2521–2525.

[9] Y. Zhang, H. Sun, F. Xu, and D. Wang, "OFDM transform-domain channel estimation based on MMSE for underwater acoustic channels," in *2008 2nd International Conference on Anti-counterfeiting, Security and Identification*, Aug 2008, pp. 177–181.

[10] D. L. Donoho, A. Maleki, and A. Montanari, "Message passing algorithms for compressed sensing: II. analysis and validation," in *2010 IEEE Information Theory Workshop on Information Theory (ITW 2010, Cairo)*, 2010, pp. 1–5.

[11] I. Daubechies, M. Defrise, and C. Mol, "An iterative thresholding algorithm for linear inverse problems with a sparsity constrains," *Communications on Pure and Applied Mathematics*, vol. 57, 11 2004.

[12] L. Wan, X. Qiang, L. Ma, Q. Song, and G. Qiao, "Accurate and efficient path delay estimation in OMP based sparse channel estimation for OFDM with equispaced pilots," *IEEE Wireless Commun. Lett.*, vol. 8, no. 1, pp. 117–120, 2019.

[13] S. Liu, F. Yang, W. Ding, X. Wang, and J. Song, "Two-dimensional structured-compressed-sensing-based NBI cancelation exploiting spatial and temporal correlations in MIMO systems," *IEEE Trans. Veh. Technol.*, vol. 65, no. 11, pp. 9020–9028, 2016.

[14] G. Qiao, X. Qiang, L. Wan, and Y. Xiao, "Chirp Z-transform based sparse channel estimation for underwater acoustic OFDM in clustered channels," in *OCEANS 2018 MTS/IEEE Charleston*, 2018, pp. 1–6.

[15] S. Liu, L. Xiao, Z. Han, and Y. Tang, "Eliminating NB-IoT interference to LTE system: A sparse machine learning-based approach," *IEEE Internet Things*, vol. 6, no. 4, pp. 6919–6932, 2019.

[16] T. T. Do, L. Gan, N. Nguyen, and T. D. Tran, "Sparsity adaptive matching pursuit algorithm for practical compressed sensing," in *2008 42nd Asilomar Conference on Signals, Systems and Computers*, 2008, pp. 581–587.

[17] S. Liu, F. Yang, C. Zhang, and J. Song, "Narrowband interference mitigation based on compressive sensing for OFDM systems," *IEICE Trans. Fund. Elect. Commun. Comp. Sci.*, vol. E98-A, pp. 870–873, 03 2015.

[18] S. Banerjee and M. Agrawal, "On the performance of underwater communication system in noise with Gaussian mixture statistics," in *2014 Twentieth National Conference on Communications (NCC)*, 2014, pp. 1–6.

[19] S. Liu, F. Yang, W. Ding, and J. Song, "Double kill: Compressive-sensing-based narrow-band interference and impulsive noise mitigation for vehicular communications," *IEEE Trans. Veh. Technol.*, vol. 65, no. 7, pp. 5099–5109, 2016.

[20] S. Liu, L. Xiao, L. Huang, and X. Wang, "Impulsive noise recovery and elimination: A sparse machine learning based approach," *IEEE Trans. Veh. Technol.*, vol. 68, no. 3, pp. 2306–2315, 2019.

[21] M. Borgerding, P. Schniter, and S. Rangan, "AMP-inspired deep networks for sparse linear inverse problems," *IEEE Trans. Signal Process.*, vol. 65, no. 16, pp. 4293–4308, 2017.

[22] J. Li, Q. Zhang, X. Xin, Y. Tao, Q. Tian, F. Tian, D. Chen, Y. Shen, G. Cao, Z. Gao, and J. Qian, "Deep learning-based massive MIMO CSI feedback," in *2019 18th International Conference on Optical Communications and Networks (ICOCN)*, 2019, pp. 1–3.

[23] Q. Bai, J. Wang, Y. Zhang, and J. Song, "Deep learning-based channel estimation algorithm over time selective fading channels," *IEEE Trans. Cognit. Commun. Netw.*, vol. 6, no. 1, pp. 125–134, 2020.

[24] M. Zhou, J. Wang, H. Sun, J. Qi, X. Feng, and H. Esmaiel, "A novel DNN based channel estimator for underwater acoustic communications with IM-OFDM," in *2020 IEEE International Conference on Signal Processing, Communications and Computing (ICSPCC)*, 2020, pp. 1–6.

[25] B. Li, S. Zhou, M. Stojanovic, L. Freitag, and P. Willett, "Multicarrier communication over underwater acoustic channels with nonuniform Doppler shifts," *IEEE J. Ocean. Eng.*, vol. 33, no. 2, pp. 198–209, 2008.

[26] C. R. Berger, S. Zhou, J. C. Preisig, and P. Willett, "Sparse channel estimation for multicarrier underwater acoustic communication: From subspace methods to compressed sensing," *IEEE Trans. Signal Process.*, vol. 58, no. 3, pp. 1708–1721, 2010.

[27] M. Stojanovic, "Low complexity OFDM detector for underwater acoustic channels," in *OCEANS 2006*, 2006, pp. 1–6.

[28] P. Qarabaqi and M. Stojanovic, "Statistical characterization and computationally efficient modeling of a class of underwater acoustic communication channels," *IEEE J. Ocean. Eng.*, vol. 38, no. 4, pp. 701–717, 2013.

[29] M. Borgerding and P. Schniter, "Onsager-corrected deep learning for sparse linear inverse problems," in *2016 IEEE Global Conference on Signal and Information Processing (GlobalSIP)*, 2016, pp. 227–231.